

# High sensitivity of strong-field multiple ionization to conical intersections

Vladimir S. Petrovic<sup>1,2,\*</sup>, Sebastian Schorb<sup>3</sup>, Jaehee Kim<sup>1,2</sup>, James White<sup>2,4</sup>, James P. Cryan<sup>1,2,3</sup>, J. Michael Glowonia<sup>2,3,4</sup>, Lucas Zipp<sup>1,2,3</sup>, Douglas Broege<sup>2,3,4</sup>, Shungo Miyabe<sup>2,5</sup>, Hongli Tao<sup>2,5</sup>, Todd Martinez<sup>2,3,5</sup>, Philip H. Bucksbaum<sup>1,2,3,4</sup>

<sup>1</sup>Stanford University, Department of Physics, Stanford, CA

<sup>2</sup>The Stanford PULSE Institute, Menlo Park, CA

<sup>3</sup>SLAC National Accelerator Laboratory, Menlo Park, CA

<sup>4</sup>Stanford University, Department of Applied Physics, Stanford, CA

<sup>5</sup>Stanford University, Department of Chemistry, Stanford, CA

Nonradiative energy dissipation in electronically excited polyatomic molecules proceeds through conical intersections, loci of degeneracy between electronic states. Here we demonstrate a high sensitivity of strong-field multiple ionization to conical intersections. By measuring kinetic energy of ions resulting from time-resolved strong-field fragmentation of isomerizing 1,3-cyclohexadiene, we separated out the time dependence of strong-field double ionization rate. A delayed enhancement in the double ionization rate correlates with molecular geometry corresponding to a degeneracy between the HOMO and LUMO orbitals. Strong-field multiple ionization is generally applicable to investigation of non-radiative processes.

Nonradiative relaxation of electronic excitation in polyatomic molecules proceeds via conical intersections [1], loci of degeneracy between different electronic states. The Born-Oppenheimer approximation, which is suitable for describing a molecule in equilibrium geometry, breaks down in the vicinity of conical intersections. When that occurs, the equations describing motion of electrons and nuclei become coupled, leading to difficulties in computation of the molecular dynamics. Due to a ubiquity of conical intersections, there has been a lot of effort to develop suitable theoretical frameworks and new experimental techniques for their direct probing [1]. In this article we discuss a particular sensitivity of strong-field multiple ionization to conical intersections, and claim that strong-field ionization can serve as a generally applicable probe of non-radiative dynamics.

Intense laser fields can initiate molecular fragmentation through multiple ionization followed by a repulsion of the remaining positive charges [2]. The ability of the molecular fragmentation to report on a chemical transformation in time-resolved experiments depends on the difference in the fragmentation patterns between the starting material and the transient species or product. Such time-

---

\* petrovic@stanford.edu

resolved fragmentation experiments have been used to follow wavepacket motion [2] and study unimolecular reactions [3, 4].

Photoinitiated ring opening of 1,3-cyclohexadiene (CHD) to form 1,3,5-hexatriene (HT) is a paradigmatic example of a unimolecular reaction that occurs through a conical intersection between two electronic states ( $S_1$  and  $S_0$ ). The molecule has been extensively studied [3-12] (for a recent review see [13] and the references therein), and is suitable for testing new experimental techniques. Ion fragment time-of-flight (TOF) mass spectra of the parent molecule CHD and the product HT differ significantly when short intense 800 nm radiation is used for fragmentation [3, 4, 14]. The HT isomer is characterized by a more violent fragmentation that leads to an increase of smaller-mass fragments, particularly  $H^+$ , compared to that of CHD. This qualitative difference between the CHD and HT fragmentation TOF mass spectra has been used in time-resolved experiments to monitor the CHD ring opening [3, 4].

In the experiment reported here, we were able to distinguish fragmentation channels originating from  $CHD^{n+}$  ions of different charges by measuring the kinetic energy of different fragment groups. This is an advantage for probing the  $S_1/S_0$  conical intersection in CHD over the past measurements, which only monitored the evolution of the ion-TOF spectra upon photoexcitation. In those experiments signals corresponding to fragmentation channels originating from decomposition of the ions with different charges were overlapped. Measurement of the kinetic energy for different ion fragment groups enabled us to separate the time-dependence of the rates for competing processes and relate them to the molecular geometry change during the isomerization. In particular, the rate for double ionization proved particularly sensitive to the HOMO/LUMO degeneracy that underlies the nonradiative energy relaxation in CHD through isomerization.

To investigate the sensitivity of the strong-field multiple ionization to conical intersections, we initiated the CHD isomerization by a short UV pulse (266 nm,  $\sim 120$  fs,  $< 10 \mu J$ ). The excitation launches a wavepacket on a spectroscopically bright  $S_2$  potential energy surface that rapidly crosses onto the  $S_1$  surface and accelerates to the  $S_1/S_0$  conical intersection. We monitored the wavepacket crossing of the  $S_1/S_0$  conical intersection via time-resolved fragmentation initiated by an intense IR field (800 nm,  $\sim 80$  fs,  $100 \mu J$ ). Kinetic energy of different ion fragment groups, separated by their travel times, was measured in steps of 30 fs over  $\sim 1.5$  ps. We gated differentiated  $H^+/H_2^+$ ,  $CH_n^+$ ,  $C_2H_n^+$ ,  $C_3H_n^+$ ,  $C_4H_n^+$ ,  $C_5H_n^+$  and  $C_6H_n^+$  fragment groups without the ability to distinguish individual peaks within each group.

### Results and discussion

Figure 1 shows the ion kinetic energy dependence on the time delay between the UV pump pulse and the IR fragmentation probe pulse, plotted separately for different ion fragment groups. Two sets of fragments, differentiated by their kinetic energy, are visible in  $C_2H_n^+$ ,  $C_3H_n^+$ , and  $C_4H_n^+$  ion groups. We refer to these sets in further discussion as 'low kinetic energy' ( $\sim 1$  eV) and 'high kinetic energy' (2 - 12 eV) sets. In other ion groups only one of the two sets is apparent. This is the case in  $H^+$  and  $CH_n^+$  groups that display only the high kinetic energy fragment sets, and  $C_6H_n^+$  group where only the low kinetic energy fragment set is observed. In some cases a partial overlap prevents a better separation of different kinetic energy sets.

This is the case in  $C_5H_n^+$ , where the peak of the distribution is at lower kinetic energy, but a long tail persists at higher kinetic energies.

Separation of ion fragments into the high and low kinetic energy groups allows us to infer the ionic charge of  $CHD^{n+}$  at the onset of the fragmentation. We estimate that, depending on the location of the charges at the onset of fragmentation, the kinetic energy divided between two fragments in the fragmentation of  $CHD^{2+}$  ranges from 5-13 eV (respectively, for limiting cases of two positive charges located on two farthestmost carbons 2.9 Å apart, or neighboring C and H atoms separated by 1.1 Å). The kinetic energies of the high kinetic energy fragment groups in  $H^+$ ,  $CH_n^+$ ,  $C_2H_n^+$ ,  $C_3H_n^+$ , and  $C_4H_n^+$  suggest that these ions are formed by fragmentation of  $CHD^{2+}$  (excluding a very weak peak in  $CH_n^+$  at 8.2 eV, not visible in the color scheme of the Fig. 1, likely originating from  $CHD^{3+}$ ). In fragmentation of a doubly charged ion the heavier fragment is released with less kinetic energy. This agrees with a decrease in the separation between the low and high kinetic energy peaks, and is likely responsible for the shape of the radial distribution of  $C_5H_n^+$ . The low kinetic energy in fragment sets visible in the  $C_2H_n^+$ ,  $C_3H_n^+$ ,  $C_4H_n^+$ ,  $C_5H_n^+$ , and  $C_6H_n^+$  groups suggest that these ion fragments resulted from a dissociation of excited  $CHD^+$ , which can be formed by multiple single- and two-color pathways.

Time dependence for the integrated signals belonging to higher and lower kinetic energy fragment groups are plotted in Fig. 2. Three patterns of behavior are observable: lower kinetic energy fragments that peak at time zero (in  $C_2H_n^+$ ,  $C_3H_n^+$ , and  $C_4H_n^+$ ,  $C_5H_n^+$ ,  $C_6H_n^+$  groups), higher kinetic energy fragments that peak 150 fs after time zero (in  $H^+$ ,  $CH_n^+$ ,  $C_2H_n^+$ ,  $C_3H_n^+$ ,  $C_4H_n^+$  groups), and higher kinetic energy fragments that peak at time zero (part of  $CH_n^+$  group, possibly tail of the  $C_5H_n^+$  group). Based on their different time-dependence, and kinetic energy, we propose that three processes contribute appreciably to the signal in our experiment, one originating from decomposition of  $CHD^+$  and two from the decomposition of  $CHD^{2+}$ . These three processes are multi-photon single ionization, IR-ionization of the UV-formed  $CHD^+$  and IR double ionization of the UV-excited neutral  $CHD/HT$  system. In the next paragraphs we discuss the details of the time dependence for the rates of these three processes, and dedicate a particular attention to the IR double ionization of the UV-excited neutral  $CHD/HT$  system. We are especially interested in the highest kinetic energy fragments and we concentrate the discussion on the primary fragmentation processes.

The first process that our analysis identifies is multi-photon single ionization of  $CHD$ . This process is responsible for the low energy ionic fragments formed by predissociation of  $CHD^+$ . The singly charged parent ion with sufficient excess energy to fragment can be formed by absorption of two UV photons ( $IP_{CHD} = 8.25$  eV [13]), or by combination of the UV and IR photons (the 800 and 266 nm photons correspond to 1.55 eV and 4.65 eV, respectively). The single-color pathway contributes to the time-independent baseline signal, while the signal corresponding to two-color pathways is expected to peak at time delays when both pulses are present, as observed.

The second process that contributes to our signal is the IR-ionization of the UV-formed  $CHD^+$ . This agrees with our earlier results reported in [4], where we

observed a significant contribution from the UV-formed CHD<sup>+</sup>. The kinetic energy of the fragments produced by sequential two-color ionization corresponds to that of CHD<sup>2+</sup> fragmentation, and the prompt appearance of these fragments supports our assignment of this process. Large portions of the signal in the C<sub>5</sub>H<sub>n</sub><sup>+</sup> and CH<sub>n</sub><sup>+</sup> channel result from this process.

The rate of the third process displays a maximum ~150 fs after the photoexcitation. Having observed that the delayed peak occurs only in a subset of fragments, in particular those originating from the fragmentation of CHD<sup>2+</sup>, we explain the third process by enhanced strong-field double ionization by the IR pulse of the UV-excited neutral CHD/HT system. This process is responsible for the higher kinetic energy fragments observed in the H<sup>+</sup>, C<sub>2</sub>H<sub>n</sub><sup>+</sup>, C<sub>3</sub>H<sub>n</sub><sup>+</sup>, C<sub>4</sub>H<sub>n</sub><sup>+</sup> ion groups, and to some extent signal in the C<sub>5</sub>H<sub>n</sub><sup>+</sup> and CH<sub>n</sub><sup>+</sup> ion groups. An experiment reported in [15] finds that kinetic energy release, averaged over *all* of the fragments, goes through a delayed maximum before reaching the value corresponding to the CHD and HT mixture at late times [15]. That maximum is absent when x-rays are used to initiate the fragmentation [15], suggesting that a strong-field process is responsible for the delayed enhancement. This supports our assignment of the third process.

We propose that the difference between the two paths for CHD<sup>2+</sup> fragmentation discussed in the second process and third process results from different intermediates. Sequential two-color double ionization proceeds through CHD<sup>+</sup>, which relaxes by a proton loss [16] to form a benzenium ion. On the other hand, CHD<sup>2+</sup> formed by single-color strong-field double ionization stabilizes by proton migration [16]. As a consequence the Coulomb repulsion fragments C<sub>6</sub>H<sub>7</sub><sup>2+</sup> in the first case, and C<sub>6</sub>H<sub>8</sub><sup>2+</sup> in the second case. As the positive charge in C<sub>6</sub>H<sub>7</sub><sup>+</sup> is distributed over five carbon atoms, the finding that C<sub>5</sub>H<sub>n</sub><sup>+</sup> and CH<sub>n</sub><sup>+</sup> are produced in the prompt high-kinetic energy data supports our attribution of this process to the sequential two-color double ionization. Ion-ion coincident fragmentation measurements could provide a more detailed account of the discussed processes.

Figure 2 shows that the rate of IR double ionization of the UV-excited CHD/HT system evolves with time delay. We explain this variation by the molecular geometry change upon the UV excitation. As the geometry changes, the energy of the HOMO and LUMO orbitals changes, going through a degeneracy that underlies the S<sub>1</sub>/S<sub>0</sub> conical intersection. Previous experiments and theoretical models that have investigated this conical intersection report that the wavepacket launched by the UV pulse passes through the conical intersection approximately 140 fs after the photoexcitation [3, 13, 17]. We propose that when the two orbitals from which the electrons are removed in the double ionization become degenerate, the double ionization rate gets strongly enhanced. Enhanced double ionization leads to an overall increase in fragmentation, manifested as an increase in abundance of lower-mass fragments and an increase in the fragment kinetic energy. Indeed, previous work on CHD isomerization [4, 14] also reports that proton ejection goes through a delayed maximum, before reaching the value corresponding to the CHD and HT mixture at late times. The persistent high kinetic energy of lower-mass fragments suggests that the double ionization rate remains higher after the maximum compared to that of CHD. This is expected from the resonance in the HT<sup>+</sup> ion for absorption of 800 nm [18].

A similar enhancement in proton ejection has been reported to occur in strong-field fragmentation of acetylene in the ground state [19]. Theoretical model discussed in that work proposes a mechanism in which a near-degeneracy of the HOMO and HOMO-1 orbitals, which occurs in the limit of strong-field extended C-H bonds, enhances the multiple ionization that results in proton detachment. In the acetylene example [19] the degeneracy between the two orbitals from which the electrons are removed by the strong field, HOMO and HOMO-1, comes from the C-H bond elongation by the intense laser field. In CHD the degeneracy of the HOMO and LUMO orbitals for a particular geometry exists even in zero field, but it is expected that the strong-field parameters have an effect on the characteristics of the delayed enhancement [20]. Indeed, in the experiment reported here the delayed peak occurs 150 fs after the cross correlations, while earlier experiments report delays of up to 200 fs. We plan to further explore the effect of the strong field parameters on the orbital degeneracy and its potential for control over nonradiative relaxation.

Both our work and the account reported in Ref. [19] support the findings of Roither et al. who find that proton ejection is a dominant fragmentation channel in strong-field ionization of small hydrocarbons [21]. In the light of these new findings we propose that the observation of the energetic protons in the strong-field fragmentation of small hydrocarbons is a part of a more general phenomenon – sensitivity of the strong-field multiple ionization to valence orbital degeneracies. The enhanced multiple ionization in the vicinity of conical intersections leads to an increase in fragmentation, which is in the previous examples manifested as a rise in the proton abundance. Protons, as the lightest fragments, depart with highest kinetic energy and show a particularly marked change upon the onset of the double ionization. In the experiment discussed here, we report that some of the other ions follow the same pattern as  $H^+$ .

### Conclusions

We demonstrate that strong field multiple ionization accompanies valence orbital degeneracies, which underlie non-radiative energy transfer processes. In particular, measurement of kinetic energy release for different fragments in a time-resolved manner enables separation of rates for competing processes in strong-field ionization. Time evolution of these rates provides information about the structural change that the molecule is undergoing. Time-dependence of the rate for strong-field multiple ionization is thus a direct and sensitive probe of inter-orbital degeneracy responsible for the presence of conical intersections in polyatomic molecules. In CHD the increase in the double ionization rate in the vicinity of the conical intersection leads to an increase in the release of energetic fragments during the fragmentation. Specifically, the proton channel shows a notable change upon the onset of double ionization. Our work supports the findings reported in [19, 21] that the release of the energetic protons is a general feature of the strong-field fragmentation of small hydrocarbons.

Theoretical modeling of the observed enhancement in the double ionization rate requires models that can treat strong-field two-electron dynamic processes. Such *ab initio* models are difficult even for atoms. The dominant processes in the interaction between atoms and strong laser fields are explained in a framework that

uses a single active electron [22-24]. This is the case for non-sequential double ionization as well, where the first emitted electron accumulates enough kinetic energy in the ponderomotive potential of the strong laser field to eject a second electron during a rescattering [25]. Such rescattering may play a role in the explanation of the double ionization enhancement described here, but we cannot rule out a process that requires a breakdown of the single electron approximation. Previously reported quantum resonance rings [20], which arise from strong-field dressing of the crossing states in the vicinity of conical intersections, potentially play an additional role. Future experiments that benefit from higher time resolution and variation of the strong-field laser parameters will help provide mechanistic explanation of the enhanced strong-field multiple ionization in the vicinity of conical intersections. As conical intersections constitute the primary channel for nonradiative relaxation in polyatomic molecules [1], we expect that the method described here will find a widespread use in investigations of molecular structure and dynamics.

#### METHODS SUMMARY

The experiment was performed in the gas-phase, with an effusive source of CHD. The two mutually perpendicularly polarized laser beams were collinear, both being perpendicular to the molecular propagation axis. 266 nm radiation was produced by two-stage nonlinear mixing of 800 nm pulses. Ions were collected by a velocity map imaging (VMI) detector (already described in [15]) with the following voltages applied to the repeller plate, extractor plate and flight tube, respectively: 1960 V, 1600 V, 1000 V. A portion of the electric field applied to the front of the micro-channel plate detector was temporally gated in order to separate different fragments based on their travel times. The detector axis was perpendicular to the plane defined by the laser beams and the molecular propagation axis. The images were recorded by a Thorlabs DC210 camera (640x480 pixels). At each delay we collected 200 shots. Based on the fluctuations in the ion count in the raw signal, we estimate the relative standard error of our measurement to be on the order of 4%. After picking the centroids of the hits on the detector, and centering of the averaged velocity map images we inverted them using the onion peeling algorithm [26]. This procedure was performed for all of the ion fragment groups, except for the  $C_6H_n^+$  group, where the ion count was too large to permit the centroid-picking algorithm to work and instead raw images were averaged, centered, and inverted. The kinetic energy axis was calibrated based on a SIMION calculation for the experimental geometry. The accuracy of the measurement of lower kinetic energy fragments is limited by lower efficiency of our microchannel plates close to the center of the detector, as well as imperfections in the VMI focusing, image centering, and the inversion algorithm. The inability to perform the ion-hit centroid finding in the case of the parent ion due to a high-count rate contributes to the error of the kinetic energy measurement in that case.

#### Contributions

VSP and PHB designed the experiment and wrote the manuscript. JPC and JMG designed and built the VMI detector. JLW wrote data acquisition software. VSP,

SS, JK, JLW, DB, and PHB collected the data. LZ performed the energy calibration. VSP analyzed the data. SM, HT and TM modeled excited state dynamics.

### Acknowledgements

This work was supported by the National Science Foundation. Some of the collaborators in this paper received their support through the SLAC National Accelerator Laboratory, Office of Basic Energy Sciences, U.S. Department of Energy. We thank Christoph Bostedt, John Bozek, and Markus Gühr for assistance with the VMI detector.

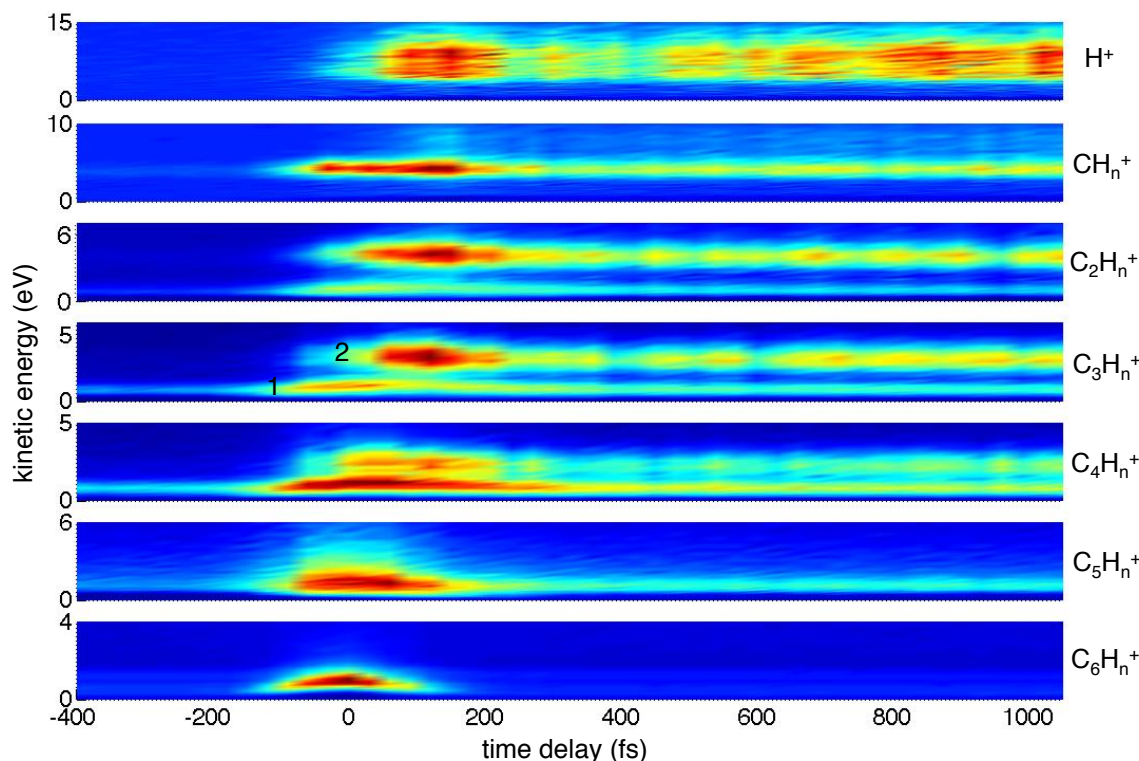


Fig. 1 Dependence of the kinetic energy of  $\text{H}^+$ ,  $\text{CH}_n^+$ ,  $\text{C}_2\text{H}_n^+$ ,  $\text{C}_3\text{H}_n^+$ ,  $\text{C}_4\text{H}_n^+$ ,  $\text{C}_5\text{H}_n^+$  and  $\text{C}_6\text{H}_n^+$  fragment groups on the time delay between the UV and IR pulses (blue represents low count, red high count; color scale differs between plots). Low and high kinetic energy sets are labeled 1 and 2, respectively, in the case of  $\text{C}_3\text{H}_n^+$ .

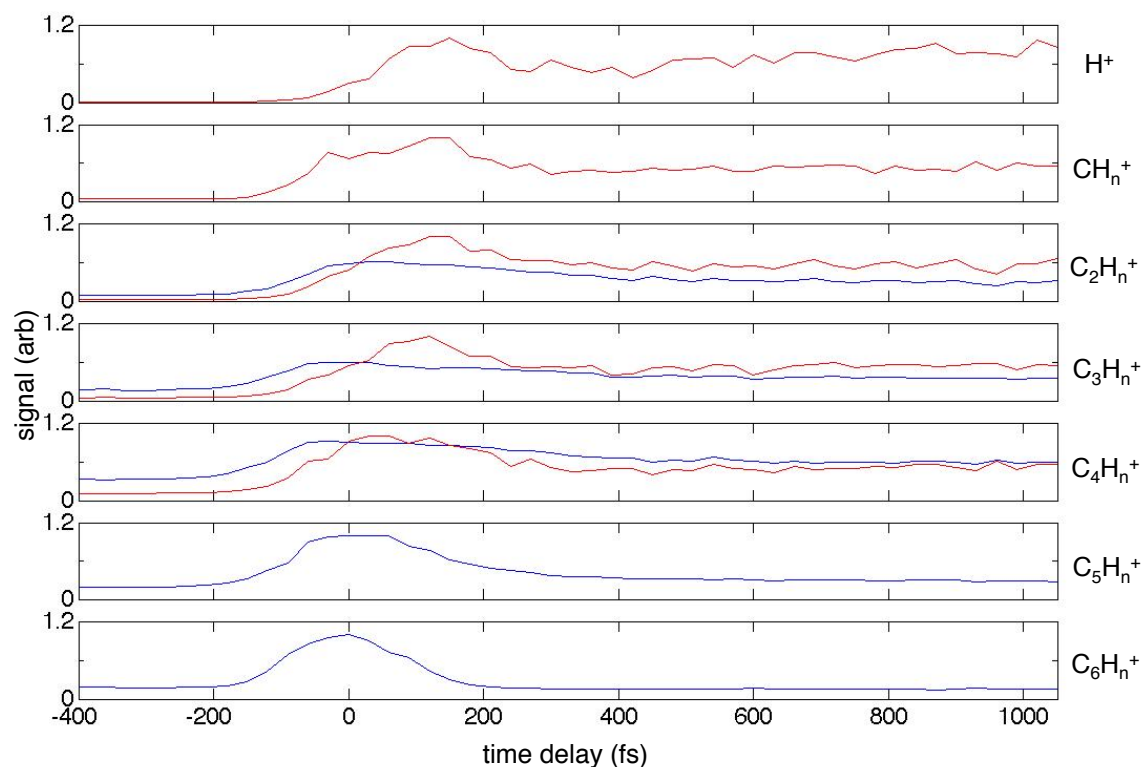


Fig. 2 Traces of integrated signal for 'low' (blue) and 'high' kinetic energy (red) sets in  $\text{H}^+$ ,  $\text{CH}_n^+$ ,  $\text{C}_2\text{H}_n^+$ ,  $\text{C}_3\text{H}_n^+$ ,  $\text{C}_4\text{H}_n^+$ ,  $\text{C}_5\text{H}_n^+$  and  $\text{C}_6\text{H}_n^+$  fragment groups.

- [1] W. Domcke, D. Yarkony, and H. Köppel, *Conical Intersections: Electronic Structure, Dynamics & Spectroscopy*, World Scientific, 2004.
- [2] C. Ellert, H. Stapelfeldt, E. Constant, H. Sakai, J. Wright, D. Rayner, and P. Corkum, *Philosophical Transactions of the Royal Society A: Mathematical, Physical and Engineering Sciences* 356 (1998) 329.
- [3] K. Kosma, S. Trushin, W. Fuß, and W. Schmid, *Physical Chemistry Chemical Physics* 11 (2009) 172.
- [4] J. L. White, J. Kim, V. S. Petrović, and P. H. Bucksbaum, *The Journal of Chemical Physics* 136 (2012) 054303.
- [5] M. Merchan, L. Serrano-Andres, L. Slater, B. Roos, R. McDiarmid, and X. Xing, in *J. Phys. Chem. A*, Vol. 103, 1999, p. 5468.
- [6] S. Pullen, N. Anderson, L. II, and R. Sension, in *J. Chem. Phys.*, Vol. 108, 1998, p. 556.
- [7] M. Kotur, T. Weinacht, B. Pearson, and S. Matsika, *The Journal of Chemical Physics* 130 (2009) 134311.
- [8] H. Ihee, V. Lobastov, U. Gomez, B. Goodson, R. Srinivasan, C. Ruan, and A. Zewail, *Science* 291 (2001) 458.
- [9] C. Ruan, V. Lobastov, R. Srinivasan, B. Goodson, H. Ihee, and A. Zewail, *Proceedings of the National Academy of Sciences* 98 (2001) 7117.



- [10] A. Hofmann, L. Kurtz, and R. de Vivie-Riedle, *Applied Physics B: Lasers and Optics* 71 (2000) 391.
- [11] P. Celani, F. Bernardi, M. Robb, and M. Olivucci, in *J. Phys. Chem*, Vol. 100, 1996, p. 19364.
- [12] H. Tamura, S. Nanbu, T. Ishida, and H. Nakamura, *The Journal of Chemical Physics* 124 (2006) 084313.
- [13] S. Deb and P. Weber, *Annual Review of Physical Chemistry* 62 (2011) 19.
- [14] S. Trushin, W. Fuß, T. Schikarski, W. Schmid, and K. Kompa, *The Journal of Chemical Physics* 106 (1997) 9386.
- [15] V. Petrović, M. Siano, J. White, N. Berrah, C. Bostedt, J. Bozek, D. Broege, M. Chalfin, R. Coffee, J. Cryan, L. Fang, J. Farrell, L. Frasinski, J. Glowonia, M. Gühr, M. Hoener, D. Holland, J. Kim, J. Marangos, T. Martinez, B. McFarland, R. Minns, S. Miyabe, S. Schorb, R. Sension, L. Spector, R. Squibb, H. Tao, J. Underwood, and P. Bucksbaum, *Physical Review Letters* 108 (2012) 253006.
- [16] T. S. Zyubina, A. M. Mebel, M. Hayashi, and S. H. Lin, *Physical Chemistry Chemical Physics* 10 (2008) 2321.
- [17] H. Tao, *First Principles Molecular Dynamics and Control of Photochemical Reactions*, Ph.D. Thesis, Stanford University 2011
- [18] H. Harada, S. Shimizu, T. Yatsushashi, S. Sakabe, Y. Izawa, and N. Nakashima, *Chemical Physics Letters* 342 (2001) 563.
- [19] E. Lötstedt, T. Kato, and K. Yamanouchi, *Physical Review A* 85 (2012)
- [20] J. Kim, H. Tao, J. L. White, V. S. Petrović, T. J. Martinez, and P. H. Bucksbaum, *The Journal of Physical Chemistry A* 116 (2011) 2758.
- [21] S. Roither, X. Xie, D. Kartashov, L. Zhang, M. Schöffler, H. Xu, A. Iwasaki, T. Okino, K. Yamanouchi, A. Baltuska, and M. Kitzler, *Physical Review Letters* 106 (2011) 163001.
- [22] P. B. Corkum, *Physical Review Letters* 71 (1993) 1994.
- [23] T. Brabec, *Strong field laser physics*, Springer, 2008.
- [24] C. Cornaggia and P. Hering, *Journal of Physics B: Atomic, Molecular and Optical Physics* 31 (1999) L503.
- [25] B. Sheehy, R. Lafon, M. Widmer, B. Walker, L. F. Dimauro, P. A. Agostini, and K. C. Kulander, *Physical Review A* 58 (1998) 3942.
- [26] G. Roberts, J. Nixon, J. Lecointre, E. Wrede, and J. Verlet, *Review of Scientific Instruments* 80 (2009) 053104.